Fish and Shellfish Immunology 87 (2019) 235–242

Contents lists available at ScienceDirect

Fish and Shellfish Immunology

journal homepage: www.elsevier.com/locate/fsi

Full length article

Transcriptome and metabolome analyses of *Coilia nasus* in response to Anisakidae parasite infection

Kai Liu[a,b], Denghua Yin[b], Yilin Shu[a], Pei Dai[b], Yanping Yang[b], Hailong Wu[a,*]

[a] Key Laboratory of Biotic Environment and Ecological Safety in Anhui Province, College of Life Sciences, Anhui Normal University, Wuhu, Anhui, 241000, China
[b] Scientific Observing and Experimental Station of Fishery Resources and Environment in the Lower Reaches of the Changjiang River, Ministry of Agriculture and Rural Affaris, Freshwater Fisheries Research Center, CAFS, WuXi, 214081, China

ARTICLE INFO

Keywords:
Coilia nasus
Anisakidae
Transcriptome
Metabolome
Immune responses
Metabolic changes

ABSTRACT

Parasites from the family Anisakidae are capable of infecting a range of marine fish species worldwide. *Coilia nasus*, which usually feeds and overwinters in coastal waters and spawns in freshwater, is highly susceptible to infection by Anisakidae. In this study, we used scanning electron microscopes to show that *C. nasus* infected by Anisakidae exhibited damage and fibrosis of the liver tissue. To better understand host immune reaction and metabolic changes to Anisakidae infection, we used a combination of transcriptomic and metabolomic method to characterize the key genes and metabolites, and the signaling pathway regulation of *C. nasus* infected by Anisakidae. We generated 62,604 unigenes from liver tissue and identified 391 compounds from serum. Of these, Anisakidae infection resulted in significant up-regulation of 545 genes and 28 metabolites, and significant down-regulation of 416 genes and 37 metabolites. Seventy-four of the 961 differentially expressed genes were linked to immune response, and 1, 2-Diacylglycerol, an important immune-related metabolite, was significantly up-regulated after infection. Our results show activation of antigen processing and presentation, initiation of the T cell receptor signaling pathway, disruption of the TCA cycle, and changes to the amino acid and Glycerolipid metabolisms, which indicate perturbations to the host immune system and metabolism following infection. This is the first study describing the immune responses and metabolic changes in *C. nasus* to Anisakidae infection, and thus improves our understanding of the interaction mechanisms between *C. nasus* and Anisakidae. Our findings will be useful for future research on the population ecology of *C. nasus*.

1. Introduction

The estuarine tapertail anchovy (*Coilia nasus*), also known as the anadromous Japanese grenadier anchovy, is distributed in the Yangtze River, the coastal waters of China and Korea, and the Ariake Sound of Japan [1–6]. *C. nasus* is the most important species for fishing and consumption in the lower reaches of the Yangtze River, China. Over the past decades, aquatic environmental pollution and overfishing have resulted in a dramatic decline in populations of *C. nasus*. The annual catch now is only about 2% of the historical maximum.

C. nasus usually feeds and overwinters in coastal areas. In the spring, individuals migrate along the Yangtze River and up to its adjacent lakes to spawn, and return to the sea after spawning [2,7–9]. During its coastal period, *C. nasus* is highly susceptible to infection by eating food that is infected with Anisakidae parasites [10–12]. Parasites from the family Anisakidae are known worldwide due to their parasitism of marine fish in the East China Sea and the Yellow Sea, and the implications to human health as the causative agents of anisakiosis [13–15]. Their life cycle comprises invertebrates and fish as intermediate or transport hosts and marine mammals or birds as definitive hosts [12,16].

The increasing influence of some parasites on fish health and the economic relevance of parasites to aquaculture and fisheries have enhanced the need for studies on fish/parasite relationships, including the immune response [17–20]. To control parasite infections, fish activate both innate and adaptive immune responses. Several mechanisms described for mammalian parasites have also been demonstrated in teleosts fishes [17,21,22]. Parasitation alters host behavior, damages tissue, affects ingestion, decreases weight, hampers reproduction, and can even cause death in some cases [23–27].

Previous studies on the effects of parasites on anadromous species have focused on the investigation of parasites. There is a lack of information on immune response, and no reports on the immune response of *C. nasus* infected by parasites. Integrated studies of omics data, such

* Corresponding author. College of Life Sciences, Anhui Normal University, No.1 Beijing East Road, Wuhu, Anhui province, China.
E-mail address: whlong@mail.ahnu.edu.cn (H. Wu).

https://doi.org/10.1016/j.fsi.2018.12.077
Received 13 September 2018; Received in revised form 18 December 2018; Accepted 31 December 2018
Available online 03 January 2019
1050-4648/

as transcriptome and metabolome analyses, have been performed to gain a comprehensive understanding of biological responses in cells and organs [28,29]. In order to illustrate the immune responses and metabolic changes that are engaged in host defense against Anisakidae infection, we compare transcriptomic and metabolomic differences between non-infected and Anisakidae-infected *C. nasus*. Understanding the interaction between *C. nasus* and Anisakidae will be useful for future research on the population ecology of *C. nasus*.

2. Materials and methods

2.1. Ethics statement

Animal welfare and experimental procedures were carried out in accordance with the Guide for the Care and Use of Laboratory Animals (Ministry of Science and Technology of China, 2006), and were approved by the animal ethics committee of the Chinese Academy of Fishery Sciences.

2.2. Chemicals and reagents

All chemicals and solvents were analytical or HPLC grade. Water, ethanol, methanol, pyridine, n-hexane, methoxylamine hydrochloride, N, O-Bis (trimethylsilyl) trifluoroacetamide (BSTFA) with 1% trimethylchlorosilane (TMCS) were purchased from CNW Technologies GmbH (Düsseldorf, Germany), Glutaraldehyde, tert-butanol and phosphate buffer were obtained from Aladdin (Shanghai, China). Finally, 2-chloro-l-phenylalanine was obtained from Shanghai Hengchuang Biotechnology Co., Ltd. (Shanghai, China).

2.3. Experimental animals and sample preparation

During May of 2016, 53 wild, ocean-river anadromous *C. nasus* individuals (verified by otolith fingerprinting technique; unpublished) were collected in the Wuhu section of the lower Yangtze River, Anhui Province, China, and immediately dissected. Anisakidae larvae were collected from fish for morphological identification and molecular verification. All samples were immediately submerged in crushed ice to retard degradation of RNA. For each *C. nasus* individual, the liver was removed and placed in liquid nitrogen, venous blood was collected from the caudal fin into ammonium-heparinized capillary tubes, and plasma was separated by centrifugation and stored at −80 °C for subsequent analysis.

According to the infection intensity of Anisakidae, we selected fourteen (seven non-infected and seven Anisakidae-infected) female *C. nasus* for transcriptome analysis and twenty (ten non-infected and ten Anisakidae-infected) female *C. nasus* for metabolome analysis (Table S1). The intensity of infection varied from 10 to 30 per fish, and a large proportion was composed of *Anisakis pegreffii* (Table S2). The body length (± standard error) was 307.98 ± 34.56 mm and the body weight was 106.60 ± 35.32 g for all fish (n = 34) sampled in this study (Table S3).

2.4. Scanning electron microscope examination

The liver tissues collected from the *C. nasus* individuals infected by Anisakidae were transferred to physiological saline and fixed for 2d in 2.5% glutaraldehyde in 0.1 M phosphate buffer. The samples were dehydrated in ascending series of ethanol and displaced with tert-butanol. Drying was performed using vacuum freezing and the samples were sputter coated with a gold–palladium complex. The coated specimens were placed on a grid, examined in a scanning electron microscope (S−3000 N), and appropriate photomicrographs were taken.

2.5. RNA sequencing, assembly, and annotation

The total RNA of each individual fish was extracted from liver samples of both infected and control *C. nasus* using TRIzol Kit (Invitrogen, USA), following manufacturer protocol. The purity, quantity and integrity of the RNA were examined with an Aglient Bioanalyzer 2100 system (Agilent Technologies, USA), and a NanoDrop ND-2000 (NanoDrop, USA). Fourteen cDNA libraries were constructed using a TruSeq Stranded mRNA LTSample Prep Kit (Illumina, San Diego, CA, USA).

Transcriptome sequencing was carried out on an Illumina HiSeq X Ten platform (Illumina, San Diego, CA, USA) that generated about 100 bp paired-end raw reads. After removing adaptor sequences, poly-N contained reads (N% > 10%), and low-quality sequences (quality score ≤ 20), the remaining clean reads were assembled using Trinity software as described for de novo transcriptome assembly without a reference genome. The assembled transcriptome was annotated using five public databases, including Nr (non-redundant), KOG (Clusters of Orthologous Groups), Swiss-Prot (protein sequences), KEGG (Kyoto Encyclopedia of Genes and Genomes), and GO (Gene Ontology).

2.6. Analysis of differentially expressed genes

To analyze Anisakidae infection, transcript expression levels were calculated in FPKM (fragments per kilobase per million mapped reads) which measures the read density normalized for RNA length and total number of reads in each sample. Genes with adjusted p values less than 0.05 and absolute value of fold changes greater than 2 were defined as differentially expressed genes (DEGs). The DEGs were subjected to KEGG and GO analyses. We determined the p value threshold using a false discovery rate (FDR), An FDR value < 0.001 indicates significant expression abundance.

Pathway-enrichment analysis identifies significantly enriched metabolic pathways or signal transduction pathways represented by differentially expressed genes. After multiple testing corrections, we considered pathways with a Q value ≤ 0.05 as significantly enriched among the differentially expressed genes. The Q value is defined as the FDR analog of the p value. The Q value of an individual hypothesis test is the minimum FDR at which the test may be called significant. Enrichment results based on NR annotation were manually checked using public databases and literature searches.

2.7. Real-time quantitative PCR validation

To validate gene expression between the control and infected groups, ten immune genes were selected (*CTSL*, *TRAF5*, *RIPK2*, *NLRP12*, *MHC2*, *ITK*, *TNFSF10*, *C3*, *CIITA* and *P38*) and their expression was determined by quantitative real-time reverse-transcription polymerase chain reaction (qRT-PCR). The cDNA templates from the control and infected groups were synthesized using the PrimeScript® RT reagent kit (TaKaRa, Dalian, China). The SYBR Green RT-PCR assay was performed on the StepOnePlus™ Real-Time PCR System (ABI, Switzerland). The PCR primers were designed using the Beacon Designer 7.0 software (Table S4). 18S rRNA was chosen as the endogenous control to normalize each gene's expression level. The results were shown in terms of relative mRNA level as mean ± SE (n = 3). One-way analysis of variance (ANOVA) was performed on the data using SPSS 22.0; differences between groups were considered statistical significance at p < 0.05.

2.8. Metabolomics detection

Eighty microlitre of each sample was added to a 1.5 mL Eppendorf tube with 10 μl of 2-chloro-l-phenylalanine (0.3 mg/mL) dissolved in methanol as an internal standard. QC samples were prepared by mixing aliquots of all samples into a pooled sample. An aliquot of the 150 μl supernatant was transferred to a glass sampling vial for vacuum-drying

at room temperature, and 80 μl of 15 mg/mL methoxylamine hydrochloride in pyridine was subsequently added. The resulting mixture was vortexed vigorously for 2 min and incubated at 37 °C for 90 min. Eighty microlitre of BSTFA (with 1% TMCS) and 20 μl n-hexane was added into the mixture, which was vortexed vigorously for 2 min and then derivatized at 70 °C for 60 min. The samples were held at ambient temperature for 30 min before GC-MS analysis.

The derivatized samples were analyzed on an Agilent 7890B gas chromatography system coupled to an Agilent 5977A MSD system (Agilent Technologies Inc., CA, USA). A DB-5MS fused-silica capillary column (30 m × 0.25 mm × 0.25 μm, Agilent J & W Scientific, Folsom, CA, USA) was utilized to separate the derivatives. Helium (> 99.999%) was used as the carrier gas at a constant flow rate of 1 mL/min through the column. The injector temperature was maintained at 260 °C. Injection volume was 1 μl by splitless mode, and the solvent delay time was set to 5 min. The initial oven temperature was 60 °C, ramped to 125 °C at a rate of 8 °C/min, to 210 °C at a rate of 5 °C/min, to 270 °C at a rate of 10 °C/min, to 305 °C at a rate of 20 °C/min, and finally held at 305 °C for 5 min. The temperature of MS quadrupole and electron impact ion source was set to 150 °C and 230 °C, respectively. The collision energy was 70 eV. Mass spectrometric data was acquired in a full-scan mode (m/z 50–500).

2.9. Analysis of differential metabolomics

The resulting GC-MS data including the peak number, sample name, and normalized peak area were imported into the SIMCA software package (14.0, Umetrics, Umea, Sweden) for Orthogonal/Partial least-squares-discriminant analysis (OPLS-DA/PLS-DA). Supervised OPLS-DA was applied to obtain a higher level of group separation and a better understanding of the variables responsible for classification. A loading plot was constructed based on the OPLS-DA, which shows the contribution of the variables to the differences between the two groups, with the important variables situated far from the origin. However, the loading plot was complex because of the high number of variables. The intercepts of R^2 and Q^2 were obtained after permutation tests with 200 iterations. The differential metabolites were selected on the basis of the combination of a statistically significant threshold of variable influence on projection values (VIP > 1) obtained from the OPLS- DA model and the p value ($p < 0.05$) from a two-tailed Student's t-test on the normalized peak areas.

3. Results

3.1. Anisakidae infection in C. nasus

C. nasus collected in the lower reaches of the Yangtze River revealed parasitic Anisakidae associated with livers and alimentary tracts (Fig. S1). As revealed by scanning electron micrograph, we found that *C. nasus* infected by Anisakidae exhibited damage to liver tissue and formation of fibrosis. Anisakidae parasites invade liver tissue of *C. nasus* in two ways: by directly penetrating the liver surface (Fig. 1A), and by generating excretory/secretory products to form grooves on the liver surface (Fig. 1B). Hepatic cells of *C. nasus* showed significant fibrosis after infection with Anisakidae (Fig. 1C); by contrast, non-infected cells appeared normal (Fig. 1D).

3.2. Transcriptome sequencing, de novo assembly and annotation

Transcript information for seven controls and seven Anisakidae infected *C. nasus* was characterized by constructing 14 cDNA libraries prepared from purified mRNA isolated from liver tissue. A total of 697,030,070 raw reads were produced, and raw sequence data were deposited into the NCBI Sequence Read Archive (SRP158758) under the NCBI Bio-project PRJNA487472. After removing low-quality and short reads, 667,898,340 clean reads corresponding to mRNAs were obtained, covering 100,108,128,818 bases (Table S5). We generated a total of 62,604 unigenes using the Trinity assembly program. The average unigene size was 1341.49 bp and the average N50 size was 1960 bp (Table S6). The length distribution of all-unigene is shown in Fig. S2. More than half of the unigenes (49,731; 79.4%) were ≥500 bp, and 27,466 unigenes were≥ 1000 bp in length. Of these, 62,604 unigenes were annotated by databases, including Nr, Swissprot, KEGG, KOG, and GO (Fig. S3). The result showed that 12.58% of genes were annotated by all five databases and 45.56% of genes were annotated by at least one public database (Table S7). The majority of the sequences showed matches with teleost fishes and a few other vertebrates. Among teleost fishes, most sequences showed similarity with *Clupea harengus* (59.81%), followed by *Pygocentrus nattereri* (2.95%), *Danio rerio* (2.28%), *Astyanax mexicanus* (2.04%), *Cyprinus carpio* (1.91%), *Salmo salar* (1.86%), and *Oncorhynchus mykiss* (1.35%). The remain sequences were classified as “others” (24.72%) (Fig. S4).

GO, an international standardized gene function classification system, classified 22,051 non-redundant unigenes into 3 categories: biological process, cellular component, and molecular function. Of the sequences categorized as “biological process”, 2062 (9.35%) and 8120 (36.82%) genes were related to immune system processes and stimulus response (Fig. S5). To classify orthologous gene products, 18,463 non-redundant unigenes were subdivided into 25 KOG functional divisions; of these, 272 genes were involved in defense mechanisms (Fig. S6). KEGG pathway analysis classified 10,282 genes into 378 specific pathways (Fig. S7). It was observed that the liver is the primary site of metabolism, with the majority of unigenes involved in this mechanism along with biosynthesis and degradation pathways. In addition, 3077 genes were enriched in pathways related to the immune system, including 588 genes in the PI3K-Akt signaling pathway, 303 genes in the NOD-like receptor signaling pathway, and 294 genes in the Chemokine signaling pathway.

3.3. Immune gene and pathway analysis

We identified 961 significantly differentially expressed genes between the control and infected groups, of which 545 genes were up-regulated and 416 genes were down-regulated after Anisakidae infection, respectively (Table D1). All of the DEGs were selected for further GO enrichment and KEGG pathways analysis, and grouped into 107 GO terms (Q value < 0.05), for the most part including immune response, adaptive immune response, inflammatory response, regulation of inflammatory response, and negative regulation of inflammatory response (Table S8). These GO terms are shown at biological process level in Fig. S8. Based on gene clustering and pathway analysis, the 74 most enriched DEGs (58 up-regulated in the infected group) were involved in specific and non-specific immunity (Fig. 2A, Table S9). The 74 DEGs were further classified into 13 significantly enriched pathways using KEGG databases (p value < 0.05; Table S10). These pathways play important roles in immunity and transcriptional regulation, such as the intestinal immune network for IgA production, Cytokine-cytokine receptor interaction, Protein digestion and absorption, and the Calcium signaling pathway (Fig. S8).

Studies have demonstrated that parasites have evolved strategies to evade host immune systems. Indeed, parasite-infected fishes exhibited significant changes in the signaling pathways related to immune response, such as TLR, complement, and chemokines [30,31]. Both GO and KEGG analyses pinpointed two important signaling pathways related to the immune system—antigen processing and presentation, and the T cell receptor signaling pathway—that were activated in Anisakidae infected *C. nasus* (Fig. 3). In addition, levels of DAG, which are implicated in the cellular immune system function, increased after the infection.

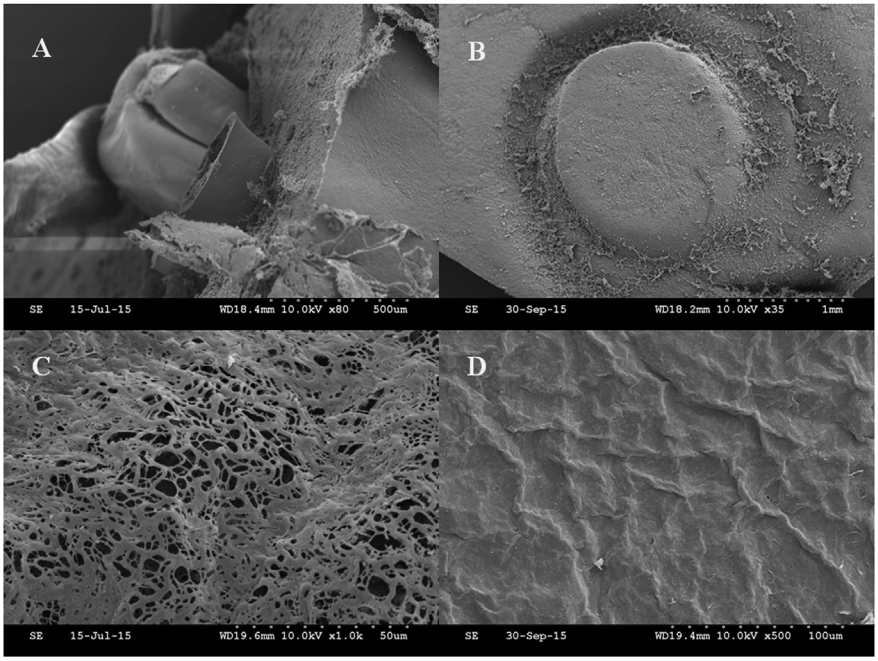

Fig. 1. Scanning electron micrograph of Anisakidae infection in *C. nasus*. (A) Penetration of liver parenchyma. (B) Formation of grooves on the liver surface. (C) Fibrosis of liver cells. (D) Normal liver cells.

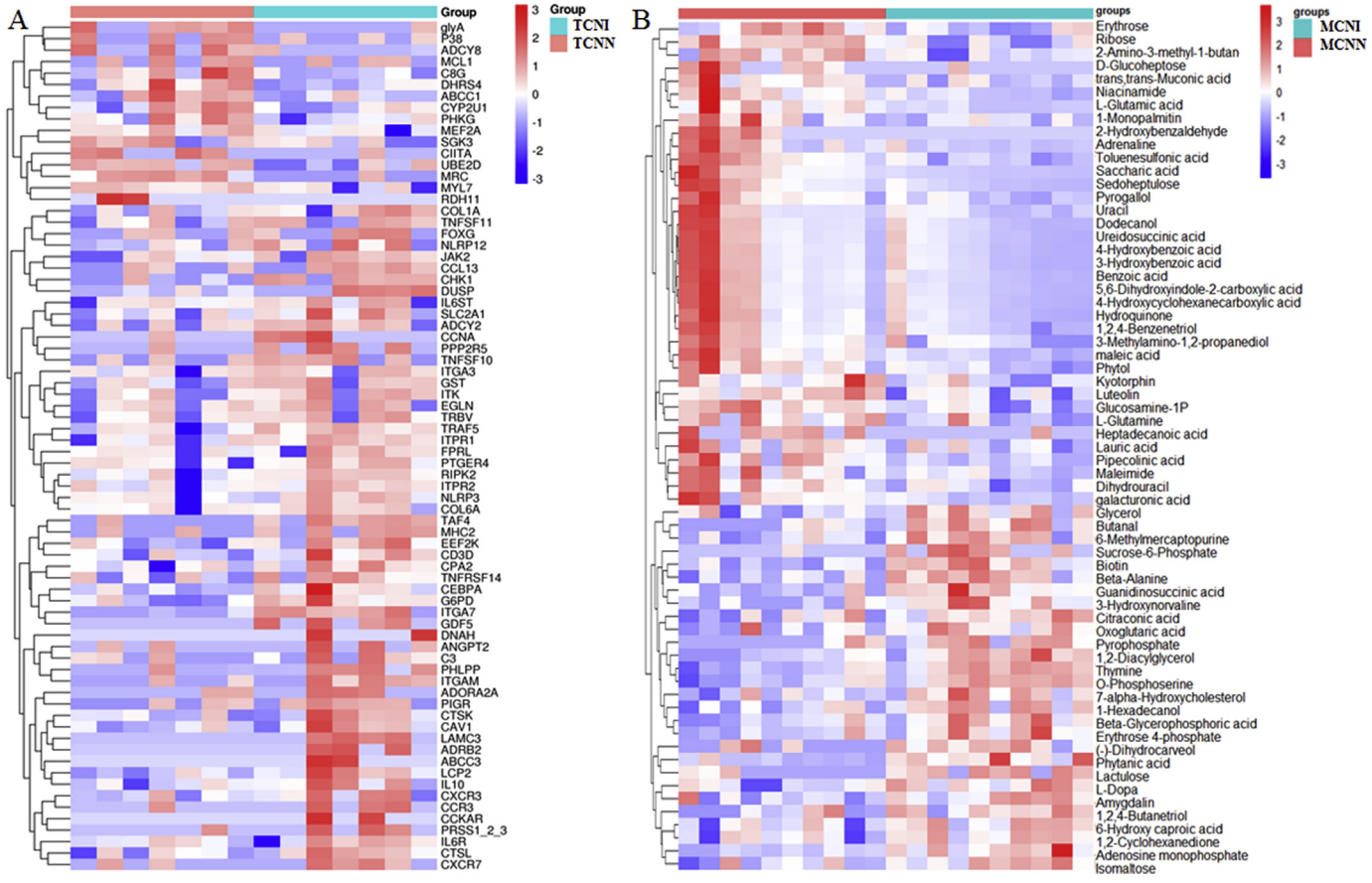

Fig. 2. Heat map of differentially expressed unigenes and metabolites. (A) Differentially expressed unigenes. (B) Differentially expressed metabolites.

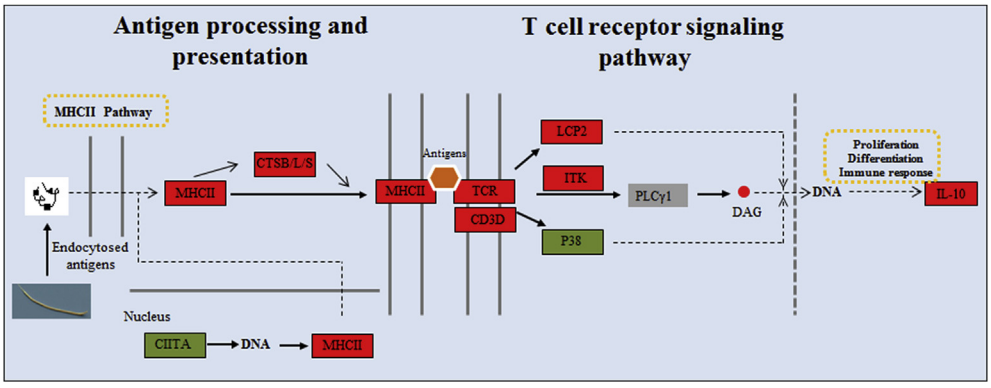

Fig. 3. Summary of major changes in the immune system of *C.nasus* in response to Anisakidae infection. The boxes indicate mRNA species, whose expression was increased (red boxes) and decreased (green boxes) after Anisakidae infection. The red circle indicates metabolites, whose expression was increased after Anisakidae infection. (For interpretation of the references to colour in this figure legend, the reader is referred to the Web version of this article.)

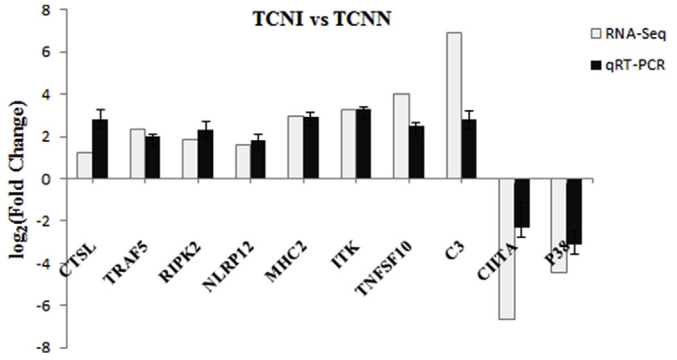

Fig. 4. Quantitative real-time RT-PCR for validation of RNA-seq. The expressions of *CTSL*, *TRAF5*, *RIPK2*, *NLRP12*, *MHC2*, *ITK*, *TNFSF10*, *C3*, *CIITA* and *P38* were detected by RNA-seq (white column) and qRT-PCR (black column).

3.4. Validation of DEGs from RNA-Seq

To examine the reliability of the DEGs identified by RNA-Seq, ten immune DEGs were chosen for analysis using qRT-PCR. Relative fold changes of qRT-PCR were compared using the RNA-Seq expression profiles. Results obtained from qRT-PCR were consistent with those of RNA-Seq, confirming the reliability of RNA-Seq data (Fig. 4).

3.5. GC-MS analysis of metabolites from infected C. nasus and controls

To assess the capability of the GC/MS-based metabolomic approach to differentiate Anisakidae infected *C. nasus* from controls, we first analyzed all total ion chromatograms of homogenized serum samples. As shown in Fig. S9, the total ion chromatograms exhibited a stable retention time without obvious drifts in their peaks. We reliably annotated 391 compounds across broad chemical classes from the serum spectra (Table D2). Twenty-eight metabolites were significantly up-regulated and 37 were significantly down-regulated between control and infected groups (Fig. 2B). Corresponding quantitative data concerning these identified metabolites is summarized in Table S11. The metabolites included amino acids, nucleotide derivatives, phospholipids, and immune-related metabolites such as 1, 2-Diacylglycerol (DAG) and Guanidinosuccinic acid.

Multivariate analyses of the serum metabolite profiles showed good separations between infected and non-infected samples. OPLS-DA and PLS-DA among the control and infected samples were performed and the two-dimensional score plots are shown in Fig. S10. OPLS-DA was conducted to determine if the Anisakidae infection influenced the metabolic pattern. The score plots for the OPLS-DA model showed clear separation between the control and Anisakidae infected groups. Supervised PLS-DA analysis sharpened the discrimination between control and infected groups. The OPLS-DA model had a multiple correlation coefficient (R^2) of 99.8% and a cross-validated predictive ability (Q^2) of 74.5%. The results showed that the infected samples were clustered closely to each other and were separated from the control samples, confirming the stability and reproducibility of the GC-MS analysis.

3.6. Metabolic pathways in Anisakidae infected C. nasus

To explore the potential metabolic pathways that were affected by Anisakidae infection, the biological roles of differentially expressed metabolites were determined by pathway analysis using MetaboAnalyst 3.0. Twenty-four pathways involving at least one annotated metabolite were screened as potential primary target pathways of interest relating to the infection (Table S12). Among these pathways, six perturbed

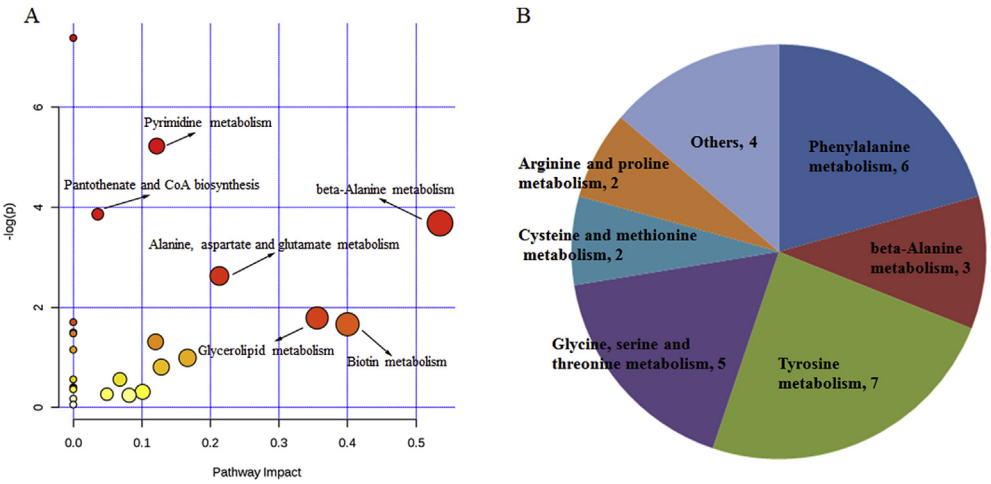

Fig. 5. Pathway analysis of the identified differential metabolites between control and Anisakidae infected *C.nasus*. (A) Pathway impact resulting from the differential metabolites using MetaboAnalyst 3.0. A small p value and big pathway impact factor indicate that the pathway is greatly influenced. (B) Distribution of differential metabolites involved in amino acid metabolism.

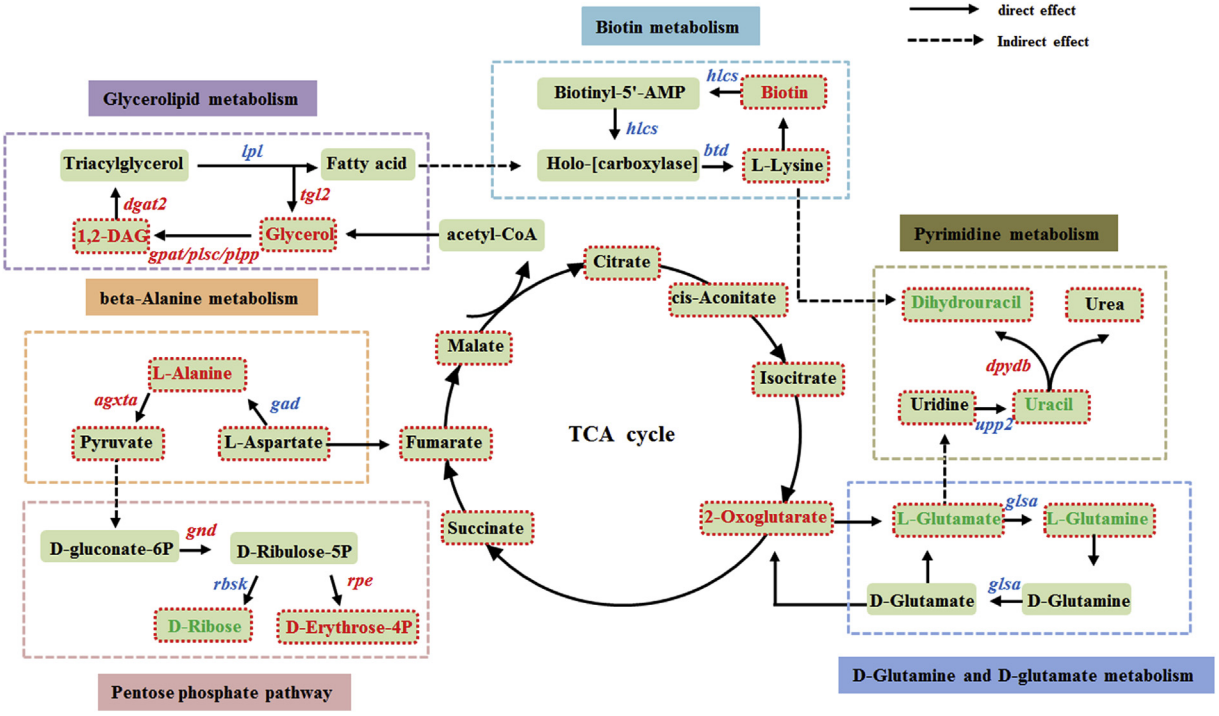

Fig. 6. Summary of major changes in *C.nasus* metabolism in response to Anisakidae infection. Compounds with red, dashed borders are metabolites that were identified in this data set. Of these, red text indicates compounds that were significantly increased, and blue text indicates compounds that were significantly decreased between control and infected samples. Text in italic font indicates mRNA species whose expression was increased (red text) or decreased (blue text) after Anisakidae infection. (For interpretation of the references to colour in this figure legend, the reader is referred to the Web version of this article.)

metabolic pathways had lower p values and higher pathway impact between control and Anisakidae infected *C. nasus* (Fig. 5A). These included pathways related to metabolism of beta-Alanine, Alanine, aspartate and glutamate, Pyrimidine, Glycerolipid, Pantothenate and CoA biosynthesis, and Biotin. Interestingly, DAG is found to be involved in Glycerolipid metabolism. Metabolism and biosynthesis of several amino acids were significantly perturbed during Anisakidae infection (Fig. 5B). A comprehensive account of metabolic changes in Anisakidae-infected *C. nasus* is shown in Fig. 6, including the involvement of the TCA cycle, Pentose phosphate pathway, Glycerolipid, beta-Alanine, Biotin, Pyrimidine, d-Glutamine and d-Glutamate metabolism.

4. Discussion

Parasites acquire resources from their hosts. The hosts utilize their energy reserves to avoid the negative impact of parasitism through investments in energetically demanding immunological responses [32]. Excretory and secretory (ES) compounds produced by parasites have several functions during infection, e.g. facilitating penetration of host tissues, and evasion of host immune responses [16,33,34]. Previous studies have shown that Anisakidae can penetrate their host's alimentary tract and invade various tissues [35,36]. In this study, we observed that some liver tissues of *C. nasus* infected by Anisakidae were seriously damaged. Microscopic observation showed that Anisakidae invade liver tissue of *C. nasus* by penetration and by forming grooves. These results indicate that parasitic Anisakidae may cause substantial damage to important tissues of *C. nasus*, which may provoke immune response.

To date, a few substantial studies were obtained and several recognitions came into consensus on the response of fish to parasite infection [17,18,21]. Meanwhile, the parasite fauna of anadromous fish has been predominately investigated on morphological and molecular analysis [37–40], but have neglected transcriptome and metabolome analyses. In order to increase ecological knowledge of an anadromous fish and to measure the parasitic impact on the host's condition, we comprehensively investigated the immune response mechanism and metabolic changes in Anisakidae-infected *C. nasus* using integrated transcriptome and metabolome analyses.

4.1. Functional analysis of immune-related genes and signaling pathways

In the transcriptome data of this study, we identified 961 DEGs in the Anisakidae infected group. GO enrichment analysis of these DEGs found that immune-related terms were the most enriched. In accordance with the above results, the heat map of the listed 74 representative immune genes also showed more up-regulated genes, and higher fold-changes of these up-regulated genes were found in infected *C. nasus* compared to the controls. In this study, all of the samples were collected, once infection intensity was visible to the naked eye, which may account for the significant up- and down-regulation of these immune genes. In our future work, we will consider the dynamic relationship between these immune genes and the parasite infection.

Antigen processing and presentation are essential elements of adaptive immunity in teleost fishes. Antigens are processed and presented to specific lymphocytes when bound to major histocompatibility complex (MHC) I and II [41–43]. In this study, we found three immune-related genes involved in antigen processing and presentation—*TRBV* (annotated as T cell receptor beta chain V region), *MHC II* (major histocompatibility complex class II), and *CTSL* (cathepsin L). MHC-II molecules presented antigenic fragments acquired by the endocytic route to the immune system for recognition and activation of $CD4^+$ T cells [44]. $CD4^+$ T cells are critical for controlling parasite infection in fish [17,45]. Cathepsin L has been found in rock bream [46] and orange-spotted grouper [47], and functions as a barrier against pathogen invasion. Five genes in the T cell receptor signaling pathway —*TRBV*, *CD3D* (T-cell surface glycoprotein CD3 delta chain), *LCP2* (lymphocyte cytosolic protein 2), *ITK* (IL2-inducible T-cell kinase) and *IL10* (interleukin 10)—were all significantly up-regulated after Anisakidae infection. Activation of T lymphocytes requires the involvement of the T cell receptor (TCR) as well as costimulatory molecules such as *CD3D* (T-cell surface glycoprotein CD3 delta chain) [48]. *TCR* functions in both

antigen recognition and signal transduction, which are crucial initial steps of antigen-specific immune responses [49]. *Itk* (IL2-inducible T-cell kinase), a Tec family tyrosine kinase, facilitates T cell receptor (TCR)-dependent calcium influxes and increases in extracellular regulated kinase activity [50]. These results suggest that the infection response of these functional molecules may defend against Anisakidae infection. However, the expression of *CIITA* (MHC class II transactivator) and *p38* (p38 MAP kinase) declined in *C. nasus* livers after Anisakidae infection, which suggests that the parasite adopted a strategy that impairs the host's antigen processing and presentation, which may facilitate chronic infection by decreasing T cell responses to antigens [51].

Interestingly, DAG, as well as important immune metabolites, plays a vital role in antigen presentation and T cell activation. DAG is critical for driving the activation, proliferation, migration, and effector function of adaptive and innate immune cells. The generation of DAG can be accomplished by the activation of various cell-surface receptors, such as TCR [52]. Taken together, our results demonstrate that the two immune pathways and their regulator were crucial candidate genes and metabolites in invoking the immune response against Anisakidae infection.

4.2. Metabolic changes of C. nasus to Anisakidae infection

Our results indicate that infection-specific patterns were acquired in the serum metabolomics profile and that they can be used to distinguish *C. nasus* infected by Anisakidae from the non-infected *C. nasus*. In addition, 65 putative metabolites were identified, and pathway analysis revealed many metabolites that were involved in metabolic pathways. The accumulation of 2-Oxoglutarate in our study suggests that the TCA cycle functioning of the host was affected by Anisakidae infection. The TCA cycle is a key metabolic pathway in all aerobic organisms that generates energy through oxidation of fuel molecules (e.g. glucose, fatty acids and certain amino acids) into carbon dioxide [53,54]. Studies have shown that T cell activation requires considerable energy and cellular resources [55,56]. As revealed by transcriptome analyses, the T cell receptor signaling pathway was activated in response to infection. These results suggest that the change of 2-Oxoglutarate in the TCA cycle may be associated with host immune responses against Anisakidae infection. In addition, 2-Oxoglutarate can be converted by Glutamate with subsequent formation of NADPH [57,58]. Similarly, NADPH production is also an important outcome of the pentose phosphate pathway [59]. Generally, pyruvate that can be transferred from the cytoplasm into the mitochondrion connects the pentose phosphate pathway to the TCA cycle [58]. NADPH has multiple functions in immune cells and is used by NADPH oxidase to generate reactive oxygen species (ROS). ROS production is a general protective mechanism employed by most organisms against stressors, such as parasites or pathogens [60]. In total, these results suggest that resistance to Anisakidae infection causes changes to the TCA cycle and to the pentose phosphate pathway.

Pathway analysis also revealed that biological functions of amino acids played important roles in the response to Anisakidae infection. Amino acids can be used as fuel by the immune system either directly, or following their conversion to other amino acids (e.g., glutamine) or to glucose [61]. The increased levels of beta-alanine indicate liver impairment [62]. Glutamine is a key compound in cellular metabolism, and low levels could be the result of the inflammatory response in reaction to an infection [63–65]. Therefore, the elevated levels of beta-alanine in infected *C. nasus* may suggest tissue damage caused by Anisakidae infection. Interestingly, the decrease of Glutamine in infected *C. nasus* may be relevant to the host surviving Anisakidae infection. These results also suggest that diverse disruptions of the amino acid metabolism occur in *C. nasus* when resisting Anisakidae infection.

Parasitism induces changes in the amounts of lipids within the host, including enhancing metabolism of fat body triacylglycerols and a higher level of free fatty acids in the haemolymph [66–68]. Metabolites of DAG and glycerol in the Glycerolipid metabolism were up-regulated after Anisakidae infection. The gene responsible for their synthesis, diacylglycerol O-acyltransferase 2 (*dgat2*), was also significantly up-regulated in infected *C. nasus*. DGAT enzymes play fundamental roles in the metabolism of diacylglycerol (DAG), and triacylglycerol (TAG) that are involved in many aspects of physiological functions, such as signal transduction, adipose tissue formation, satiety, and lactation [69]. These results suggest that resistance to Anisakidae infection causes changes to Glycerolipid metabolism.

5. Conclusion

The integration of transcriptome and metabolome profiling showed that Anisakidae infection resulted in several major perturbations to the host immune responses and to metabolic changes, including activation of antigen processing and presentation, initiation of the T cell receptor signaling pathway, disruption of the TCA cycle, and changes to the amino acid and Glycerolipid metabolisms. This study provides important knowledge of the interaction mechanisms between *C. nasus* and Anisakidae, which will be useful for future research on the population ecology of *C. nasus*. Although this study has achieved a deeper understanding of the immune responses and metabolic changes to *C. nasus* infected by Anisakidae, there are still many unanswered questions. In the future studies, we will carry out further investigation of *C. nasus* population ecology and Anisakidae infection, collect more detailed infection data, investigate tissue injury from Anisakidae infection, and explore the effects of parasitic Anisakidae on the anadromous *C. nasus* for better understandings of parasitic Anisakidae on population structure and recruitment of *C. nasus*.

Compliance with ethical standards

Conflicts of interest

The authors declare that they have no conflict of interest.

Acknowledgements

This study was supported by the Agricultural finance special project "Investigation of fishery resources and environment in the lower Yangtze River" (CJDC-2017-22), Ministry of agriculture's species resources conservation project (Investigation and analysis of special catch resources, 2017), and Aquatic life and fishery environmental monitoring key station (downstream station) monitoring project of the three gorges project of the Yangtze river (JJ[2017]-010).

Appendix A. Supplementary data

Supplementary data to this article can be found online at https://doi.org/10.1016/j.fsi.2018.12.077.

References

[1] T. Jiang, J. Yang, X.Q. Shen, Life history of Coilia nasus from the Yellow Sea inferred from otolith Sr:Ca ratios, Environ. Biol. Fish. 95 (2012) 503–508.
[2] G. Zhu, L. Wang, W. Tang, D. Liu, J. Yang, De novo transcriptomes of olfactory epithelium reveal the genes and pathways for spawning migration in Japanese grenadier anchovy (Coilia nasus), PLoS One 9 (8) (2014-8-1) e103832 2014 9.
[3] F. Du, G. Xu, Z. Nie, P. Xu, R. Gu, Transcriptome analysis gene expression in the liver of Coilia nasus during the stress response, BMC Genomics 15 (1) (2014-07-04) 558 2014 15.
[4] H. Shen, R. Gu, G. Xu, P. Xu, Z. Nie, Y. Hu, In-depth transcriptome analysis of Coilia ectenes , an important fish resource in the Yangtze River: de novo assembly, gene annotation, Mar Genomics 23 (2015) 15–17.
[5] J.R. Duan, Y.F. Zhou, D.P. Xu, M.Y. Zhang, K. Liu, Y. Shi, et al., Ovary transcriptome profiling of Coilia nasus during spawning migration stages by Illumina sequencing, Marine Genomics 21 (2015) 17–19.
[6] Y.F. Zhou, J.R. Duan, K. Liu, D.P. Xu, M.Y. Zhang, D.A. Fang, et al., Testes transcriptome profiles of the anadromous fish Coilia nasus during the onset of spermatogenesis, Marine Genomics 24 (2015) 241–243.
[7] G. Zhu, L. Wang, W. Tang, X. Wang, C. Wang, Identification of olfactory receptor

genes in the Japanese grenadier anchovy Coilia nasus, Genes & Genomics 39 (2017) 521–532.
[8] G. Xu, F. Du, L. Yan, Z. Nie, P. Xu, Integrated application of transcriptomics and metabolomics yields insights into population-asynchronous ovary development in Coilia nasus, Sci. Rep. 6 (2016) 31835.
[9] S. Rui, X. Wen, Li, G. Shan, Hong Z. Wu, T. Gui, Wang, Population genetic structure of the acanthocephalan Acanthosentis cheni in anadromous, freshwater, and landlocked stocks of its fish host, Coilia nasus, J. Parasitol. 100 (2014) 193–197.
[10] W.X. Li, H. Zou, S.G. Wu, R. Song, G.T. Wang, Richness and diversity of helminth communities in the Japanese Grenadi, J. Parasitol. 98 (1937) 449–452.
[11] W.X. Li, R. Song, S.G. Wu, H. Zou, P. Nie, G.T. Wang, Seasonal occurrence of helminths in the anadromous fish Coilia nasus, J. Parasitol. 97 (1937) 192–196.
[12] T.M. Murphy, M. Berzano, S.M. O'Keeffe, D.M. Cotter, S.E. Mcevoy, K.A. Thomas, et al., Anisakid larvae in Atlantic salmon (Salmo salar L.) grilse and post-smolts: molecular identification and histopathology, J. Parasitol. 96 (2010) 77–82.
[13] J.W. Smith, R. Wootten, Anisakis and Anisakiasis, Adv. Parasitol. 16 (1978) 93–163.
[14] S. Mattiucci, G. Nascetti, Chapter 2 advances and trends in the molecular systematics of anisakid nematodes, with implications for their evolutionary ecology and host—parasite Co-evolutionary processes, Adv. Parasitol. 66 (2008) 47–148.
[15] M. Audicana, M. Kennedy, Anisakis simplex: from obscure infectious worm to inducer of immune hypersensitivity, Clin. Microbiol. Rev. 21 (2008) 360.
[16] F. Mehrdana, K. Buchmann, Excretory/secretory products of anisakid nematodes: biological and pathological roles, Acta Vet. Scand. 59 (2017) 42.
[17] P. Alvarez-Pellitero, Fish immunity and parasite infections: from innate immunity to immunoprophylactic prospects, Vet. Immunol. Immunopathol. 126 (2008) 171–198.
[18] B.S. Dezfuli, G. Bosi, J.A. Depasquale, M. Manera, L. Giari, Fish innate immunity against intestinal helminths, Fish Shellfish Immunol. 50 (2016) 274–287.
[19] W.C. Gause, J.F. Urban, M.J. Stadecker, The immune response to parasitic helminths: insights from murine models, Trends Immunol. 24 (2003) 269–277.
[20] B.S. Dezfuli, A. Lui, P. Boldrini, F. Pironi, L. Giari, The Inflammatory Response of Fish to Helminth Parasites vol. 15, (2008), pp. 426–433.
[21] A. Sitjà-Bobadilla, I. Estensoro, J. Pérez-Sánchez, Immunity to gastrointestinal microparasites of fish, Dev. Comp. Immunol. 64 (2016) 187–201.
[22] R.M. Anthony, L.I. Rutitzky, UJ Jr., M.J. Stadecker, W.C. Gause, Protective immune mechanisms in helminth infection, Nat. Rev. Immunol. 7 (2007) 975.
[23] J.D. Williams, C.B. Boyko, The global diversity of parasitic isopods associated with crustacean hosts (Isopoda: Bopyroidea and Cryptoniscoidea), PLoS One 7 (2012) e35350.
[24] K.A. Hadfield, N.L. Bruce, N.J. Smit, Review of the fish-parasitic genus Cymothoa Fabricius, 1793 (Isopoda, Cymothoidae, Crustacea) from the southwestern Indian Ocean, including a new species from South Africa, Zootaxa 3640 (2013) 152.
[25] T.,. Horton, B. Okamura, Cymothoid isopod parasites in aquaculture: a review and case study of a Turkish sea bass (Dicentrarchus labrax) and sea bream (Sparus auratus) farm, Dis. Aquat. Org. 46 (2001) 181–188.
[26] C.A. Neves, M.P. Pastor, L.E. Nery, E.A. Santos, Effects of the parasite Probopyrus ringueleti (Isopoda) on glucose, glycogen and lipid concentration in starved Palaemonetes argentinus (Decapoda), Dis. Aquat. Org. 58 (2004) 209–213.
[27] E.P. Papapanagiotou, J.P. Trilles, Cymothoid parasite Ceratothoa parallela inflicts great losses on cultured gilthead sea bream sparus aurata in Greece, Dis. Aquat. Org. 45 (2001) 237–239.
[28] S.Y. Cho, Y.K. Kwon, M. Nam, B. Vaidya, S.R. Kim, S. Lee, et al., Integrated profiling of global metabolomic and transcriptomic responses to viral hemorrhagic septicemia virus infection in olive flounder, Fish Shellfish Immunol. 71 (2017) 220.
[29] G. Xu, F. Du, Y. Li, Z. Nie, P. Xu, Integrated application of transcriptomics and metabolomics yields insights into population-asynchronous ovary development in Coilia nasus, Sci. Rep. 6 (2016) 31835.
[30] F. Tian, C. Tong, C. Feng, K. Wanghe, K. Zhao, Transcriptomic profiling of Tibetan highland fish (Gymnocypris przewalskii) in response to the infection of parasite ciliate Ichthyophthirius multifiliis, Fish Shellfish Immunol. 70 (2017).
[31] P. Ronza, D. Robledo, R. Bermúdez, A.P. Losada, B.G. Pardo, A. Sitjà-Bobadilla, et al., RNA-seq analysis of early enteromyxosis in turbot (Scophthalmus maximus): new insights into parasite invasion and immune evasion strategies, Int. J. Parasitol. 46 (2016) 507–517.
Slavík et al., 2017 O. Slavík, P. Horký, K. Douda, J. Velíšek, J. Kolářová, P. Lepič, Parasite-induced increases in the energy costs of movement of host freshwater fish, Physiol. Behav. 171 (2017) 127–134.
[33] Q.Z. Bahlool, A. Skovgaard, P.W. Kania, K. Buchmann, Effects of excretory/secretory products from Anisakis simplex (Nematoda) on immune gene expression in rainbow trout (Oncorhynchus mykiss), Fish Shellfish Immunol. 35 (2013) 734–739.
[34] F. Mehrdana, P.W. Kania, S. Nazemi, K. Buchmann, Immunomodulatory effects of excretory/secretory compounds from Contracaecum osculatum larvae in a zebrafish inflammation model, PLoS One 12 (2017) e0181277.
[35] Q.Z. Bahlool, A. Skovgaard, P. Kania, S. Haarder, K. Buchmann, Microhabitat preference of Anisakis simplex in three salmonid species: immunological implications, Vet. Parasitol. 190 (2012) 489–495.
[36] E.,. Abollo, C.,. Gestal, S. Pascual, Anisakis infestation in marine fish and cephalopods from Galician waters: an updated perspective, Parasitol. Res. 87 (2001) 492–499.
[37] S. Mele, M.G. Pennino, M.C. Piras, D. Macías, M.J. Gómez-Vives, F. Alemany, et al., Ecology of the Atlantic black skipjack Euthynnus alletteratus (Osteichthyes: scombridae) in the western Mediterranean Sea inferred by parasitological analysis, Parasitology 143 (2016) 1330–1339.
[38] C. Gérard, M. Hervé, M. Gay, O. Bourgau, E. Feunteun, A. Acou, et al., Metazoan parasite communities in Alosa alosa (Linnaeus, 1758) and Alosa fallax (Lacépède, 1803) (Clupeidae) from North-East Atlantic coastal waters and connected rivers, Parasitol. Res. 116 (2017) 1–20.
[39] A. Confer, V. Vu, C.J. Drevecky, W.E. Aguirre, Occurrence of Schistocephalus solidus in anadromous threespine stickleback, J. Parasitol. 98 (2012) 676.
[40] I M, JA D, M N, CW B, I L, P J, et al., The influence of aquaculture unit proximity on the pattern of Lepeophtheirus salmonis infection of anadromous Salmo trutta populations on the isle of Skye, Scotland, J. Fish. Biol. 92 (2018) 1849–1865.
[41] A.N. Vallejo, N.W. Miller, N.E. Harvey, M.A. Cuchens, G.W. Warr, L.W. Clem, Cellular pathway(S) of antigen processing and presentation in fish APC: endosomal involvement and cell-free antigen presentation, Dev. Immunol. 3 (2014) 51–65.
[42] M.V. Jatin, G.VdV. Annemarthe, L.P. Hidde, The known unknowns of antigen processing and presentation, Nat. Rev. Immunol. 8 (2008) 607–618.
[43] Q.H. Abram, B. Dixon, B.A. Katzenback, Impacts of low temperature on the teleost immune system, Biology 6 (2017).
[44] T.D.H. Van, P. Paul, M.L. Jongsma, J. Neefjes, Routes to manipulate MHC class II antigen presentation, Curr. Opin. Immunol. 23 (2011) 88–95.
[45] K. Buchmann, Fish immune responses against endoparasitic nematodes - experimental models, J. Fish. Dis. 35 (2012) 623–635.
[46] W. Ilson, D.Z. Mahanama, N. Chamilani, L. Youngdeuk, K. Yucheol, L. Sukkyoung, et al., Molecular characterization and expression analysis of Cathepsin B and L cysteine proteases from rock bream (Oplegnathus fasciatus), Fish Shellfish Immunol. 30 (2011) 763–772.
[47] J.Z. Liang, Y.Z. Rao, Z.R. Lun, T.B. Yang, Cathepsin L in the orange-spotted grouper, Epinephelus coioides: molecular cloning and gene expression after a Vibrio anguillarum challenge, Fish Physiol. Biochem. 38 (2012) 1795–1806.
[48] J.E. Smith-Garvin, G.A. Koretzky, M.S. Jordan, T cell activation, Annu. Rev. Immunol. 27 (2009) 591–619.
[49] M. Baniyash, TCR zeta-chain downregulation: curtailing an excessive inflammatory immune response, Nat. Rev. Immunol. 4 (2004) 675–687.
[50] S.C. Bunnell, M. Diehn, M.B. Yaffe, P.R. Findell, L.C. Cantley, L.J. Berg, Biochemical interactions integrating Itk with the T cell receptor-initiated signaling cascade, J. Biol. Chem. 275 (2000) 2219–2230.
[51] D. Yang, Q. Liu, M. Yang, H. Wu, Q. Wang, J. Xiao, et al., RNA-seq liver transcriptome analysis reveals an activated MHC-I pathway and an inhibited MHC-II pathway at the early stage of vaccine immunization in zebrafish, BMC Genomics 13 (2012) 319.
[52] B.K. Singh, K. Taku, The immunomodulatory functions of diacylglycerol kinase ζ, Frontiers in Cell & Developmental Biology 4 (2016).
[53] T.V. Nguyen, A.C. Alfaro, F. Merien, T. Young, R. Grandiosa, Metabolic and immunological responses of male and female New Zealand Greenshell™ mussels (Perna canaliculus) infected with Vibrio sp, J. Invertebr. Pathol. 157 (2018) 80–89.
[54] T.V. Nguyen, A.C. Alfaro, T. Young, S. Ravi, F. Merien, Metabolomics study of immune responses of New Zealand Greenshell™ mussels (Perna canaliculus) infected with pathogenic Vibrio sp, Mar. Biotechnol. 20 (2018) 396–409.
[55] D. Klysz, X. Tai, P.A. Robert, M. Craveiro, G. Cretenet, L. Oburoglu, et al., Glutamine-dependent α-ketoglutarate production regulates the balance between T helper 1 cell and regulatory T cell generation, Sci. Signal. 8 (2015) ra97.
[56] S.R. Jacobs, C.E. Herman, N.J. Maciver, J.A. Wofford, H.L. Wieman, J.J. Hammen, et al., Glucose uptake is limiting in T cell activation and requires CD28-mediated Akt-dependent and independent pathways, J. Immunol. 180 (2008) 4476.
[57] C. Ebenaujehle, M. Boll, G. Fuchs, 2-Oxoglutarate:NADP+ oxidoreductase in Azoarcus evansii: properties and function in electron transfer reactions in aromatic ring reduction, J. Bacteriol. 185 (2003) 6119.
[58] A.C. Munhoz, P. Riva, D. Simões, C. Rui, A.R. Carpinelli, Control of insulin secretion by production of reactive oxygen species: study performed in pancreatic islets from fed and 48-hour fasted wistar rats, PLoS One 11 (2016) e0158166.
[59] J. Foreman, V. Demidchik, J.H.F. Bothwell, P. Mylona, H. Miedema, M.A. Torres, et al., Reactive oxygen species produced by NADPH oxidase regulate plant cell growth, Nature 422 (2003) 442–446.
[60] L.A.J. O'Neill, R.J. Kishton, J. Rathmell, A guide to immunometabolism for immunologists, Nat. Rev. Immunol. 16 (2016) 553.
[61] P.C. Calder, Branched-chain amino acids and immunity, J. Nutr. 136 (2006) 288S.
[62] G.A. Randi, A.L. Evans, F. Åsa, M.F. Bertelsen, B. Stéphane, J.M. Arnemo, Seasonal variation in haematological and biochemical variables in free-ranging subadult brown bears (Ursus arctos)in Sweden, BMC Vet. Res. 11 (2015) 301.
[63] H. Buter, M. Koopmans, R. Kemperman, L. Jekel, C. Boerma, Plasma glutamine levels before cardiac surgery are related to post-surgery infections; an observational study, J. Cardiothorac. Surg. 11 (2016) 155.
[64] D.W. Wilmore, J.K. Shabert, Role of glutamine in immunologic responses, Chinese Journal of Chinical Nutrition 14 (1999) 618.
[65] L. Sun, L. Yi, C. Zhang, X. Liu, S. Feng, W. Chen, et al., Glutamine was required for snakehead fish vesiculovirus (SHVV) propagation via replenishing the tricarboxylic acid cycle, J. Gen. Virol. 97 (2016) 2849.
[66] Y. Nakamatsu, T. Tanaka, Venom of Euplectrus separatae causes hyperlipidemia by lysis of host fat body cells, J. Insect Physiol. 50 (2004) 267–275.
[67] M. Kaeslin, R. Pfister-Wilhelm, B. Lanzrein, Influence of the parasitoid Chelonus inanitus and its polydnavirus on host nutritional physiology and implications for parasitoid development, J. Insect Physiol. 51 (2005) 1330–1339.
[68] S. Zhang, J.Y. Luo, L.M. Lv, C.Y. Wang, C.H. Li, X.Z. Zhu, et al., Effects of Lysiphlebia japonica (Ashmead) on cotton-melon aphid Aphis gossypii Glover lipid synthesis, Insect Mol. Biol. 24 (2015) 348–357.
[69] Y. Shi, D. Cheng, Beyond triglyceride synthesis: the dynamic functional roles of MGAT and DGAT enzymes in energy metabolism, Am. J. Physiol. Endocrinol. Metabol. 297 (2009) E10.